THE JOURNAL OF BIOLOGICAL CHEMISTRY VOL. 289, NO. 10, pp. 6695–6708, March 7, 2014

Identification of Phosphatase That Dephosphorylates Xylose in the Glycosaminoglycan-Protein Linkage Region of Proteoglycans*

Received for publication, September 19, 2013, and in revised form, January 5, 2014 Published, JBC Papers in Press, January 14, 2014, DOI 10.1074/jbc.M113.520536

Toshiyasu Koike[1], **Tomomi Izumikawa**[1], **Ban Sato**[1], **and Hiroshi Kitagawa**[2]

From the Department of Biochemistry, Kobe Pharmaceutical University, Higashinada-ku, Kobe 658-8558, Japan

Background: The enzyme responsible for the dephosphorylation of xylose in glycosaminoglycans remains unknown.
Results: A protein that removed the phosphate from the phosphorylated linkage trisaccharide and localized in the Golgi was identified. Inhibition of this protein phosphatase resulted in decreased glycosaminoglycan levels in cells.
Conclusion: We identified the phosphoxylose phosphatase that regulates glycosaminoglycan synthesis.
Significance: Transient phosphorylation of xylose residues controls glycosaminoglycan synthesis.

Recently, we demonstrated that FAM20B is a kinase that phosphorylates the xylose (Xyl) residue in the glycosaminoglycan-protein linkage region of proteoglycans. The phosphorylation of Xyl residues by FAM20B enhances the formation of the linkage region. Rapid dephosphorylation is probably induced just after synthesis of the linker and just before polymerization initiates. Indeed, *in vitro* chondroitin or heparan sulfate polymerization does not occur when the Xyl residue of the tetrasaccharide linkage region is phosphorylated. However, the enzyme responsible for the dephosphorylation of Xyl remains unknown. Here, we identified a novel protein that dephosphorylates the Xyl residue and designated it 2-phosphoxylose phosphatase. The phosphatase efficiently removed the phosphate from the phosphorylated trisaccharide, Galβ1–3Galβ1–4Xyl(2-*O*-phosphate), but not from phosphorylated tetrasaccharide, GlcUAβ1–3Galβ1–3Galβ1–4Xyl(2-*O*-phosphate). Additionally, RNA interference-mediated inhibition of 2-phosphoxylose phosphatase resulted in increased amounts of GlcNAcα1–4GlcUAβ1–3Galβ1–3Galβ1–4Xyl(2-*O*-phosphate), Galβ1–3Galβ1–4Xyl(2-*O*-phosphate), and Galβ1–4Xyl(2-*O*-phosphate) in the cells. Gel filtration analysis of the glycosaminoglycan chains synthesized in the knockdown cells revealed that these cells produced decreased amounts of glycosaminoglycan chains and that the chains had similar lengths to those in the mock-transfected cells. Transcripts encoding this phosphatase were ubiquitously, but differentially, expressed in human tissues. Moreover, the phosphatase localized to the Golgi and interacted with the glucuronyltransferase-I involved in the completion of the glycosaminoglycan-protein linkage region. Based on these findings, we conclude that transient phosphorylation of the Xyl residue in the glycosaminoglycan-protein linkage region controls the formation of glycosaminoglycan chains of proteoglycans.

Chondroitin sulfate (CS)[3] and heparan sulfate (HS), like other glycosaminoglycans (GAGs), are linear polysaccharide chains and comprise repeating disaccharide units (-4GlcUAβ1–3GalNAcβ1-)$_n$ and (-4GlcUAβ1–4GlcNAcα1-)$_n$, respectively. Assembly of GAG chains is initiated with the synthesis of the common GAG-protein linkage region GlcUAβ1–3Galβ1–3Galβ1–4Xylβ1-*O*-Ser, which is attached to specific serine residues of specific core proteins. The linkage region tetrasaccharide is formed by sequential stepwise addition of monosaccharide residues by four specific glycosyltransferases as follows: xylosyltransferase (XylT), galactosyltransferase-I (GalT-I), galactosyltransferase-II (GalT-II), and glucuronyltransferase-I (GlcAT-I) (1). The repeating disaccharide region of HS is synthesized onto the linkage region by the HS co-polymerase complex comprising EXT1 and EXT2. In contrast, the repeating disaccharide region of CS is synthesized onto the linkage region by enzyme complexes of bi-functional chondroitin synthases (ChSy)-1, -2, and -3 and chondroitin polymerizing factor (ChPF) (2–5).

Previous structural analysis of the GAG-protein linkage region revealed the presence of several modifications. One such modification is the phosphorylation of the Xyl residue at position 2 (1, 6). This modification occurs in both HS and CS derived from cell-rich tissues (7, 8) and appears to affect the transfer of Gal and GlcUA residues by GalT-I and GlcAT-I, respectively (9, 10). Findings from *in vitro* experiments with authentic substrates indicate that phosphorylation of the Xyl residue prevents the transfer of a Gal residue by GalT-I (9). In contrast, GlcAT-I efficiently transfers a GlcUA residue to the phosphorylated trisaccharide *in vitro* (10). These results sug-

* This work was supported in part by Grants-in-aid for Scientific Research (B) 25293014 (to H. K.) and for Scientific Research on Innovative Areas 23110003 (to H. K.) and by the supported program for the Strategic Research Foundation at Private Universities, 2012–2016 (to H. K.), from the Ministry of Education, Culture, Sports, Science and Technology, Japan.

The nucleotide sequence(s) reported in this paper has been submitted to the GenBank™/EBI Data Bank with accession number(s)AB827640.

[1] These authors contributed equally to this work.

[2] To whom correspondence should be addressed: Dept. of Biochemistry, Kobe Pharmaceutical University, 4-19-1 Motoyamakita-machi, Higashinada-ku, Kobe 658-8558, Japan. Tel.: 81-78-441-7570; Fax: 81-78-441-7571; E-mail: kitagawa@kobepharma-u.ac.jp.

[3] The abbreviations used are: CS, chondroitin sulfate; GAG, glycosaminoglycan; HS, heparan sulfate; EXT, exostosin; ChSy, chondroitin synthase; ChPF, chondroitin polymerizing factor; ESC, embryonic stem cell; GlcUA, D-glucuronic acid; GlcAT-I, glucuronyltransferase I; shRNA, short hairpin RNA; TM, thrombomodulin; Ni-NTA, nickel-nitrilotriacetic acid; EGFP, enhanced GFP; ER, endoplasmic reticulum.

gest that phosphorylation of the Xyl residue takes place after transfer of the first Gal residue by GalT-I and before transfer of the GlcUA residue by GlcAT-I. Indeed, phosphorylation of the Xyl residue is most prominent after the addition of two Gal residues (11, 12). Transient phosphorylation of Xyl residues seems to enhance the formation of the linkage region (13–15). Subsequently, rapid dephosphorylation is probably induced just before initiation of polymerization. In fact, the formation of the disaccharide repeat regions of the HS and CS chains is initiated on dephosphorylated tetrasaccharide linkage structures (4, 16). Therefore, dephosphorylation of the Xyl residue may be required for biosynthetic maturation of the linkage region sequence, which may be a prerequisite for the initiation and efficient elongation of the repeating disaccharide region of GAG chains.

Recently, we demonstrated that the FAM20B kinase phosphorylates the Xyl residue in the linkage region (14). Overexpression of *FAM20B* increased the amount of both CS and HS in HeLa cells, whereas RNA interference of *FAM20B* resulted in a reduction of both GAGs in the cells (14). Gel filtration analysis of the GAG chains synthesized in cells overexpressing *FAM20B* revealed that the GAG chains had similar lengths to those in the mock-transfected cells. These results indicate that FAM20B regulates the number of GAG chains by phosphorylating the Xyl residue in the GAG-protein linkage region of proteoglycans. However, the enzyme responsible for the dephosphorylation of Xyl remains unknown. Here, we describe the cloning of a human cDNA encoding a novel protein capable of dephosphorylating this Xyl residue. We designated this enzyme 2-phosphoxylose phosphatase (XYLP).

EXPERIMENTAL PROCEDURES

Materials—[γ-^{32}P]ATP (3000 Ci/mmol) and [γ-^{32}P]NaH_2PO_4 (285.2 mCi/mmol) were purchased from PerkinElmer Life Sciences. UDP-GlcUA, UDP-GalNAc, and ATP (each unlabeled) were purchased from Sigma. Chondroitinase ABC (EC 4.2.2.20), chondroitinase AC-II (EC 4.2.2.5) from *Arthrobacter aurescens*, heparinase from *Flavobacterium heparinum* (EC 4.2.2.7), and heparitinase from *F. heparinum* (EC 4.2.2.8) were purchased from Seikagaku Corp. (Tokyo, Japan). β-Glucuronidase from *Ampullaria* (EC 3.2.1.31) was purchased from Wako. rAPid alkaline phosphatase, recombinant alkaline phosphatase from bovine intestine (EC 3.1.3.1), was purchased from Roche Diagnostics. α-Thrombomodulin (α-TM) with a truncated linkage region tetrasaccharide (GlcUAβ1–3Galβ1–3Galβ1–4Xyl) was purified and structurally characterized as described previously (17). Superdex Peptide HR10/30 and Superdex 200 10/300 GL columns were purchased from Amersham Biosciences.

Polymerization Assay and Identification of Polymerization Reaction Products—First, a phosphate transfer reaction was conducted as follows: GlcUAβ1–3Galβ1–3Galβ1–4Xylβ1-*O*-TM (α-TM) was used as an acceptor in each 20-μl incubation mixture, which contained 10 μl of beads bearing the soluble form of FAM20B as the enzyme source and 10 μM [γ-^{32}P]ATP (1.11×10^5 dpm), 50 mM Tris buffer, pH 7.0, 10 mM $MnCl_2$, 10 mM $CaCl_2$, and 0.1% BSA as described (14). Subsequent polymerization reactions were simultaneously incubated in parallel in 20-μl reaction mixtures containing 1 nmol of GlcUAβ1–3Galβ1–3Galβ1–4[^{32}P]Xyl(2-*O*-phosphate) β1-*O*-TM or α-TM and 0.25 mM UDP-[^{3}H]GalNAc, 0.25 mM UDP-GlcUA, 100 mM MES buffer, pH 6.5, 10 mM $MnCl_2$, and 10 μl of the soluble form of ChSy-1/ChPF-bound beads as described (4). Each mixture was incubated at 37 °C overnight, and a Superdex peptide column equilibrated with the elution buffer (0.25 M NH_4HCO_3, 7% 1-propanol) and gel filtration chromatography were used to separate the radiolabeled products. The radioactive fractions containing the enzyme reaction products were pooled, and these mixtures were dehydrated. The dried reaction products were subjected to reductive β-elimination with $NaBH_4$/NaOH, and Superdex 200 column and eluent containing 0.25 M NH_4HCO_3, 7% 1-propanol were then used to analyze the products.

Construction of a Soluble Form of 2-Phosphoxylose Phosphatase—PCR was used to amplify a cDNA fragment predicted to encode a truncated form of the putative phosphatase (XYLP) lacking the first 37 N-terminal amino acids; the template cDNA was obtained from Open Biosystems (MHS1010-7508558, corresponding to the human acid phosphatase-like-2 (ACPL2) cDNA in GenBank™ BC035834); the 5′-primer (5′-GAAGATCTGGAATGAGTAGCAAGAGTCGA-3′) contained an in-frame BglII site, and the 3′-primer (5′-GAAGATCTGTGGACCTTTCCCTATGCTCT-3′) contained a BglII site located 38 bp downstream of the predicted stop codon. PCR was performed using KOD-Plus DNA polymerase (TOYOBO, Tokyo, Japan) for 30 cycles at 94 °C for 30 s, 58 °C for 30 s, and 68 °C for 150 s in 5% (v/v) dimethyl sulfoxide. The PCR fragment was then subcloned into the BamHI site of pGIR201protA (18), thereby resulting in the fusion of the insulin signal sequence and the protein A sequence present in the vector. The sequences of the plasmid construct (pEF-BOS/IP-ACPL2) were confirmed by DNA sequencing.

Site-directed Mutagenesis—A soluble form of GlcAT-I was produced as described previously (10). A two-stage PCR mutagenesis method was used to construct an expression plasmid that encoded a soluble form of the GlcAT-I mutant. Two separate PCRs were performed to generate two overlapping gene fragments using a cDNA that encoded the soluble form of GlcAT-I as a template. In the first PCR, a sense 5′-primer (5′-GGAAGATCTCTACGGCAGGAAGGATCTGAGGAT-3′) containing a BglII site and an antisense internal mutagenic (E281A) primer (5′-GGCCACCTGGCGAGCAGTCTTCTG-3′, the mutated nucleotide is underlined) were used. In the second round of PCR, a sense internal mutagenic primer (complementary to the antisense internal mutagenic primer) and an antisense 3′-primer (5′-GGAAGATCTGATGGTGGAGAAAAGTCCGTG-3′) containing a BglII site, which was located 18 bp downstream of the stop codon, were used. These two PCR products were gel-purified and then used as the template for a third PCR amplification with the sense 5′-primer and the antisense 3′-primer described previously. The final PCR fragment was subcloned into the BamHI site of pGIR201protA (18).

Expression of a Soluble Form of Phosphatase—FuGENE 6 (Roche Diagnostics) was used according to the manufacturer's instructions to transfect pEF-BOS/IP-ACPL2 (6.0 μg) into

COS-1 cells that were growing on 100-mm plates. For co-transfection experiments, the XYLP and GlcAT-I or GlcAT-I E281A mutant expression plasmids (3.0 μg each) were co-transfected into COS-1 cells on 100-mm plates using FuGENE 6, as above. Two days after transfection, 4 ml of the culture medium was collected and incubated with 10 μl of IgG-Sepharose (Amersham Biosciences) for 12 h at 4 °C. The beads were recovered by centrifugation and washed with the assay buffer. The beads were then resuspended in the same assay buffer and tested for phosphatase activity as described below. To measure the amount of protein absorbed onto IgG-Sepharose beads, the bound protein was eluted with 1 M acetic acid, and BCA protein assay reagent (enhanced protocol, Pierce) was then used to measure protein content of the eluant.

Phosphatase Assays and Identification of Reaction Products—First, a phosphate transfer reaction was conducted. α-TM with a truncated linkage region tetrasaccharide (GlcUAβ1–3Galβ1–3Galβ1–4Xyl) (1 nmol) was used as an acceptor in each 20-μl incubation mixture, which contained 10 μl of beads bound to the soluble form of FAM20B (14) and 10 μM [γ-^{32}P]ATP (1.11 $\times$ 10^5 dpm), 50 mM Tris buffer, pH 7.0, 10 mM $MnCl_2$, 10 mM $CaCl_2$, and 0.1% BSA. Next, β-glucuronidase was used to digest the phosphorylated tetrasaccharides at 37 °C in a reaction buffer containing 50 mM NaOAc and 1 mM $MgCl_2$. Additionally, phosphorylated tetrasaccharides were used as acceptors in individual 20-μl incubation mixtures, which contained 10 μl of beads bound to a soluble form of chondroitin GalNAc transferase-1 (19) or EXTL2 (20). Then, the products of each reaction were separated by gel filtration chromatography on a Superdex peptide column that had been equilibrated with elution buffer (0.25 M NH_4HCO_3, 7% 1-propanol). The fractions containing the enzyme reaction products were pooled and dehydrated. The isolated reaction products were used as substrates for the phosphatase reactions. Phosphatase reactions were simultaneously incubated in parallel in 20-μl reaction mixtures containing 5 pmol of Galβ1–3Galβ1–4[^{32}P]-Xyl(2-*O*-phosphate)β1-*O*-TM, GlcUAβ1–3Galβ1–3Galβ1–4[^{32}P]Xyl(2-*O*-phosphate)β1-*O*-TM, GalNAcβ1–4GlcUAβ1–3Galβ1–3Galβ1–4[^{32}P]Xyl(2-*O*-phosphate)β1-*O*-TM, or GlcNAcα1–4GlcUAβ1–3Galβ1–3Galβ1–4[^{32}P]Xyl(2-*O*-phosphate)β1-*O*-TM and 50 mM Tris buffer, pH 5.8, and 10 μl of the resuspended beads or 50 mM Tris buffer, pH 8.5, 0.1 mM EDTA, 0.1% BSA, and 1 μl of rAPid alkaline phosphatase (Roche Diagnostics), recombinant alkaline phosphatase from bovine intestine expressed in *Pichia pastoris*, which was used as a control. Each of these mixtures was incubated at 37 °C for 4 h, and the products of each reaction were then separated by gel filtration chromatography on a Superdex peptide column equilibrated with the elution buffer (0.25 M NH_4HCO_3, 7% 1-propanol). Fractions (0.4 ml each) were collected at a flow rate of 0.4 ml/min, and a liquid scintillation counter was used to measure the radioactivity.

Subcellular Localization—A 5′-primer (5′-GAAGATCTG-GACATGTTCCCGAT-3′) containing a BglII site and a 3′-primer (5′-AGATCTCCGAATCCTTCCCTGTGACA-3′) containing a BglII site were used to amplify a cDNA fragment encoding XYLP. PCR was carried out with *KOD*-Plus DNA polymerase for 30 cycles at 94 °C for 30 s, 53 °C for 42 s, and 68 °C for 180 s in 5% (v/v) dimethyl sulfoxide. The PCR fragment was subcloned into the pEGFP-N1 or pDsRed-Monomer N1 expression vector (Clontech). The Golgi marker vector (pDsRed-Golgi) was constructed using the pECFP-Golgi vector (Clontech) that harbors a sequence encoding the N-terminal 81 amino acids of human β1–4-galactosyltransferase as described previously (14). The region from pECFP-Golgi was digested with NheI and BamHI and subcloned into pDsRed-Monomer N1. FuGENE 6 was used according to the manufacturer's instructions to transfect combinations of GFP-tagged and DsRed-monomer-tagged expression vectors (3.0 μg each) into HeLa cells, wild-type embryonic stem cells (ESCs), or *GlcAT-I*$^{-/-}$ ESCs (21) that were grown on glass-bottom dishes (IWAKI, Shizuoka, Japan). A laser-scanning confocal microscope LSM710 (Carl Zeiss, Tokyo, Japan) was used to obtain fluorescent images.

Construction of an Expression Vector Encoding the Phosphatase and Preparation of Stably Transfected Cells—PCR was used to amplify a cDNA fragment encoding the phosphatase (XYLP); the ACPL2 cDNA (GenBank^{TM} BC035834) was the template, and the 5′-primer (5′-GAAGATCTGGACATGTTC-CCGAT-3′) and 3′-primer (5′-GAAGATCTGTGGACTTTC-CCTA-3′) each contained a BglII site. *KOD*-Plus DNA polymerase (TOYOBO) was used to perform PCR for 30 cycles, each at 94 °C for 30 s, 53 °C for 42 s, and 68 °C for 180 s in 5% (v/v) dimethyl sulfoxide. The PCR fragments were subcloned into the BamHI site of the pCMV expression vector (Invitrogen). The sequence of each plasmid construct was confirmed by DNA sequencing. FuGENE 6 (Roche Diagnostics) was used according to the manufacturer's instructions to transfect the expression plasmid (6.0 μg) into HeLa cells that were grown on 100-mm plates. Transfectants were cultured in the presence of 300 μg/ml G418. The surviving colonies were then picked and propagated for experiments.

MISSION shRNA (Sigma) was used to inhibit XYLP expression in HeLa cells. Specifically, two constructs, each encoding hairpin RNA and isolated by the RNAi Consortium (clone number TRCN0000052898 or TRCN0000052899), were used. Each shRNA plasmid (6.0 μg) was transfected into HeLa cells on 100-mm plates by using FuGENE 6 according to the manufacturer's instructions. Transfectants were cultured in the presence of 0.4 μg/ml puromycin. Surviving colonies were then picked and propagated for experiments.

Quantitative Real Time RT-PCR—QuickPrep total RNA extraction kits (Amersham Bioscience) were used to extract total RNA from HeLa cells. Moloney murine leukemia virus-reverse transcriptase (Promega) and an oligo(dT)$_{20}$-M4 adaptor primer (Takara, Otsu, Japan) were then used to synthesize cDNA from ~1 μg of total RNA. For XYLP, the forward and reverse primers were 5′-TGTCACCAGTTCTCAGTGC-3′ and 5′-GGTGTGGAATGTGACATCG-3′, respectively; for FAM20B, the forward and reverse primers were 5′-AGAGAT-CAAACCTGTCGCC-3′ and 5′-CCAAAGTGTGACAGATC-CCT-3′, respectively; for glyceraldehyde-3-phosphate dehydrogenase, the forward and reverse primers were 5′-ATGGG-TGTGAACCATGAGAAGTA-3′ and 5′-GGCAGTGATGG-CATGGAC-3′, respectively. FastStart DNA Master plus SYBR Green I (Roche Diagnostics) and a LightCycler ST300 (Roche

Diagnostics) were used to perform quantitative real time RT-PCR. The expression level of the phosphatase transcript was normalized to that of the glyceraldehyde-3-phosphate dehydrogenase transcript.

Isolation and Purification of GAGs—Cells were homogenized in acetone and thoroughly air-dried. The dried materials were digested at 55 °C for 24 h with heat-pretreated (60 °C for 30 min) actinase E (10% by weight of dried materials) in 250 μl of 0.1 M borate sodium, pH 8.0, containing 10 mM calcium acetate. Following this digestion, each sample was adjusted to 5% trichloroacetic acid, and the resultant precipitate was removed by centrifugation. The soluble fraction was then mixed with ether. The aqueous phase was neutralized with 1.0 M sodium carbonate and adjusted to contain 80% ethanol. The resultant precipitate was dissolved in 50 mM pyridine acetate and subjected to gel filtration through a PD-10 column (Amersham Bioscience) with 50 mM pyridine acetate as an eluent. The flow-through fractions were collected and dried. Each dried sample was subsequently dissolved in water.

Analysis of Disaccharide Composition of CS and HS—Purified GAGs were digested with 5 mIU of chondroitinase ABC or a mixture of 0.5 mIU of heparinase and 0.5 mIU of heparitinase at 37 °C for 3 h. Reactions were terminated by boiling each mixture for 1 min. The digests were derivatized with the fluorophore 2-aminobenzamide, and high performance liquid chromatography (HPLC) was then used to analyze the samples as reported previously (22).

Gel Filtration Chromatography of GAGs—To measure GAG chain lengths, the purified GAGs were subjected to reductive β-elimination using $NaBH_4$/NaOH and then analyzed by gel filtration chromatography on Superdex-200 columns (10 × 300 mm) eluted with 0.2 M ammonium bicarbonate at a flow rate of 0.4 ml/min. Fractions were collected at 3-min intervals, lyophilized, and digested with chondroitinase ABC or a mixture of heparinase and heparitinase. The digests were derivatized with 2-aminobenzamide and then analyzed by HPLC on an amine-bound PA-03 column as described previously (23, 24).

Metabolic Labeling—shRNA control cells, shRNA *XYLP* cells, *FAM20B*-overexpressing cells, shRNA *FAM20B* cells (14), wild-type ESCs, or *GlcAT-I*$^{-/-}$ ESCs (21) were metabolically labeled with [^{32}P]NaH_2PO_4 (285.2 mCi/mmol) in sodium- and phosphate-free DMEM (Invitrogen) containing 10% dialyzed fetal bovine serum at 37 °C for 30 h. Each cell layer was treated with 1 mM LiOH at 4 °C for 12 h to liberate the *O*-linked saccharides from core proteins (16, 23). Each sample was subsequently neutralized and then applied to a column (1-ml bed volume) of AG 50W-X2 (H^+ form, Bio-Rad). Flow-through fractions containing *O*-linked oligosaccharide components were pooled and neutralized with 1 mM NH_4HCO_3. 2AB was used to derivatize the oligosaccharide component of the linkage region as described previously (17). The 2AB-derivatized putative linkage regions were analyzed by gel filtration chromatography on a Superdex peptide column (10 × 300 mm) eluted with 0.2 M ammonium bicarbonate at a flow rate of 0.4 ml/min. The pooled fractions were further analyzed by HPLC on an amine-bound PA-03 column in conjunction with enzymatic digestion as described previously (20, 25).

Enzyme Digestion—Each enzyme digestion was carried out with heparitinase (EC 4.2.2.8) from *F. heparinum* (3 mIU) (Seikagaku Biobusiness Corp., Tokyo, Japan), alkaline phosphatase (1 unit) (Roche Diagnostics), or chondroitinase AC-II (EC 4.2.2.5) from *A. aurescens* (10 mIU) in a total volume of 50 μl of appropriate buffer at 37 °C overnight (20, 26).

Determination of Expression Levels of XYLP and FAM20B mRNA by Real Time PCR—MTC Multiple Tissue cDNA panels were purchased from Clontech. Each panel contained first strand cDNAs from a specific human tissue, and the cDNA has been normalized against the *G3PDH* transcript. The primer pairs for *XYLP* and real time-PCR conditions were described above. The primer pair for *FAM20B* was described previously (14).

Pulldown Assays—The cDNA fragment predicted to encode a truncated form of GlcAT-I that lacks the first 43 N-terminal amino acids of GlcAT-I was amplified with a 5′-primer (5′-GCTCTAGACTACGGCAGAAGGATCTGAGGA-3′) containing an in-frame XbaI site and a 3′-primer (5′-GGAAGATCTGTGCCTGAAAAGAGGTGGTAG-3′) containing a BglII site as described previously (27). The cDNA fragment predicted to encode a truncated form of GalT-II that lacks the first 34 N-terminal amino acids of GalT-II was amplified with a 5′-primer (5′-CGGAATTCGCCGAGCCCGGGGACCCCAGG-3′) containing an in-frame EcoRI site and a 3′-primer (5′-CGGGATCCTCAGGGGATGCCCTCCCTTCT-3′) containing a BamHI site. This fragment was inserted into a pcDNA3Ins-His expression vector to encode a fusion protein with the insulin signal sequence and a His_6 sequence tag. The His-tagged and the protein A-tagged expression vectors were co-transfected into COS-1 cells grown on 100-mm plates. FuGENE™ 6 (Roche Diagnostics) was used according to the manufacturer's instructions. Two days after transfection, 1 ml of the culture medium was collected and incubated with 10 μl of Ni-NTA-agarose (Qiagen) overnight at 4 °C. The beads were recovered by centrifugation, washed with TBS buffer containing Tween 20 three times, and subjected to SDS-PAGE (7% gel); the separated proteins were transferred to a polyvinylidene difluoride (PVDF) membrane. The membrane was incubated in PBS containing 2% skim milk and 0.1% Tween 20, then incubated with IgG antibody, and then treated with anti-mouse IgG conjugated with horseradish peroxidase (Amersham Bioscience). An enhanced chemiluminescence (ECL) select detection reagent (Amersham Bioscience) was used to visualize antibody-labeled protein bands.

Statistical Analysis—Data are expressed as mean ± S.D. The Student's *t* test was used to assess statistical significance. Differences were considered significant with $p < 0.05$.

RESULTS

Phosphorylated Linkage Structure Did Not Serve as a Substrate for Chondroitin Polymerization—Xyl phosphorylation increases during Gal addition onto the linkage disaccharide, Galβ1–4Xyl, and is nearly stoichiometric at the trisaccharide level; however, GlcUA addition is accompanied by rapid Xyl dephosphorylation during decorin biosynthesis in rat skin fibroblasts (11). These results indicate that the phosphorylated linkage structure, GlcUAβ1–3Galβ1–3Galβ1–4Xyl(2-*O*-

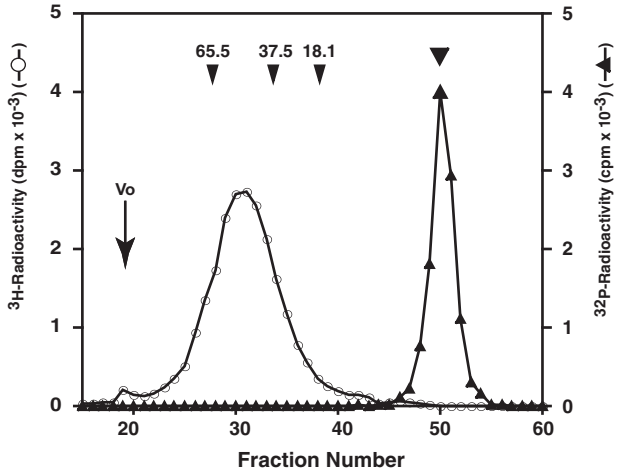

FIGURE 1. **Comparison of the chondroitin polymerization activity with phosphorylated or dephosphorylated linkage tetrasaccharides.** The ^{32}P-labeled phosphorylated tetrasaccharide linkage structure GlcUAβ1–3Galβ1–3Galβ1–4[^{32}P]Xyl(2-*O*-phosphate)β1-*O*-TM (▲) and α-TM (○) were each tested as acceptors in polymerization reactions. Each acceptor was co-expressed with the enzyme sources ChSy-1 and ChPF. ^{32}P-Labeled or [^{3}H]GalNAc-labeled polymerization reaction products were first isolated by gel filtration, next subjected to reductive β-elimination using $NaBH_4$/NaOH, and finally purified on a Superdex 200 column with 0.25 M NH_4HCO_3, 7% 1-propanol as the eluent. The *arrowheads* labeled *65.5*, *37.5*, and *18.1* indicate the elution position of the 65.5-, 37.5-, and 18.1-kDa saccharides, respectively; these molecular weight determinations were based on the elution positions of commercial polysaccharides of known sizes (dextran average M_r: 65,500, 37,500, and 18,100; all from Sigma). The *arrowhead* denote the elution position of the authentic compound, GlcUAβ1–3Galβ1–3Galβ1–4Xyl(2-*O*-phosphate).

phosphate), might markedly affect the chondroitin polymerase-mediated production of CS chains. Previously, we demonstrated that chondroitin polymerization occurs when ChSy-1 and ChPF are co-expressed, and the acceptor substrate is α-TM bearing a truncated linkage region tetrasaccharide, GlcUAβ1–3Galβ1–3Galβ1–4Xyl (5). Therefore, we investigated whether polymerization could occur on the phosphorylated linkage structure, GlcUA-Gal-Gal-Xyl(2-*O*-phosphate). We used α-TM bearing a tetrasaccharide (GlcUA-Gal-Gal-Xyl) as a primer and recombinant FAM20B as an enzyme source to generate a phosphorylated linkage structure GlcUA-Gal-Gal-[^{32}P]-Xyl(2-*O*-phosphate) attached to α-TM. This phosphorylated structure GlcUA-Gal-Gal-[^{32}P]Xyl(2-*O*-phosphate)-TM was incubated with the ChSy-1 and ChPF proteins. Polymerization did not occur when GlcUA-Gal-Gal-[^{32}P]Xyl-(2-*O*-phosphate)-TM was the acceptor substrate (Fig. 1). In addition, because we demonstrated that chondroitin polymerization is achieved by any two combinations of ChSy-1, ChSy-2, ChSy-3, and ChPF, we measured the polymerization activity using co-expression of ChSy-1/ChSy-2, ChSy-1/ChSy3, ChSy-2/ChSy-3, ChSy-2/ChPF, or ChSy-3/ChPF as the enzyme source. Polymerization did not occur with any enzyme subunit combination when GlcUA-Gal-Gal- [^{32}P]Xyl-(2-*O*-phosphate)-TM was the acceptor substrate (data not shown). These results indicated that the phosphorylated linkage structure did not serve as a substrate for chondroitin polymerization. Therefore, based on these results and the finding that the phosphorylated linkage structure is not used by HS polymerases as a substrate (20), we reasoned that dephosphorylation of the Xyl residue may be required for biosynthetic maturation of the linkage region sequence and that this maturation may be a prerequisite for the initiation and the efficient elongation of the repeating disaccharide region of GAG chains.

Identification of the Putative Phosphatase as 2-Phosphoxylose Phosphatase—Based on these findings, we propose the existence of an enzyme responsible for the dephosphorylation of Xyl. We used the query term "unidentified phosphatase-like" to search the database at the National Center for Biotechnology Information (National Institutes of Health, Bethesda) and identified a candidate protein with a type II transmembrane protein topology. The predicted gene product, designated 2-phosphoxylose phosphatase (XYLP) here (originally acid phosphatase like-2; ACPL2; GenBank^{TM} accession number AB827640), comprised 480 amino acids; this protein was predicted to have the type II transmembrane protein topology that is characteristic of all other enzymes involved in GAG biosynthesis (Fig. 2*A*). Database searches indicated that the amino acid sequence displayed weak sequence similarity to human acidic phosphatase gene family members (8.3, 22.3, and 20.1% identical to ACP1, ACP2, and ACP3, respectively) (Fig. 2*A*).

To examine whether XYLP could dephosphorylate 2-phosphoxylose within the GAG-protein linkage region, we generated a soluble form of XYLP by replacing the first 37 amino acids of XYLP with a cleavable insulin signal sequence and a protein A IgG binding domain. This soluble recombinant XYLP fusion protein was expressed in COS-1 cells. Based on Western blot analysis of culture medium, these transgenic COS-1 cells secreted a protein of ~90 kDa (Fig. 2*B*). The putative phosphatase fusion protein in the medium was purified with IgG-Sepharose beads to eliminate endogenous phosphatase; the protein-bound beads were then used as an enzyme source. We used six different substrates with variable linkage regions to assess 2-phosphoxylose phosphatase activity of the bound fusion protein. As shown in Table 1, phosphatase activity was detected with Gal-Gal-[^{32}P]Xyl(2-*O*-phosphate)-TM or GalNAc-GlcUA-Gal-Gal-[^{32}P]Xyl(2-*O*-phosphate)-TM as a substrate. Notably, no phosphatase activity was detected when GlcUA-Gal-Gal-[^{32}P]Xyl(2-*O*-phosphate)-TM or GlcNAc-GlcUA-Gal-Gal-[^{32}P]Xyl(2-*O*-phosphate)-TM was used as a substrate. Additionally, no phosphatase activity was detected using ^{32}P-osteopontin or ^{32}P-labeled matrix extracellular phosphoglycoprotein as substrates; each of these glycoproteins is phosphorylated by the Golgi kinase FAM20C (28) homologous to FAM20B (a Xyl kinase) (14). In sharp contrast, recombinant alkaline phosphatase from bovine intestine utilized all substrates examined (Table 1).

Because XYLP showed weak sequence similarity to human acidic phosphatase gene family members, the effects of pH on the enzymatic activity of XYLP were examined; Gal-Gal-[^{32}P]Xyl(2-*O*-phosphate) was used as the substrate for these assays. XYLP exhibited optimum activity at pH 5.8 (Fig. 2*C*). These findings indicated the protein secreted by the transgenic COS-1 cells was a phosphatase that dephosphorylates Xyl residues in the GAG-protein linkage region.

Subcellular Localization of XYLP—To examine the intracellular localization of Xyl phosphatase, we generated a full-length form of XYLP that carried EGFP C termini (XYLP-EGFP). XYLP-EGFP was then co-expressed with a Golgi marker

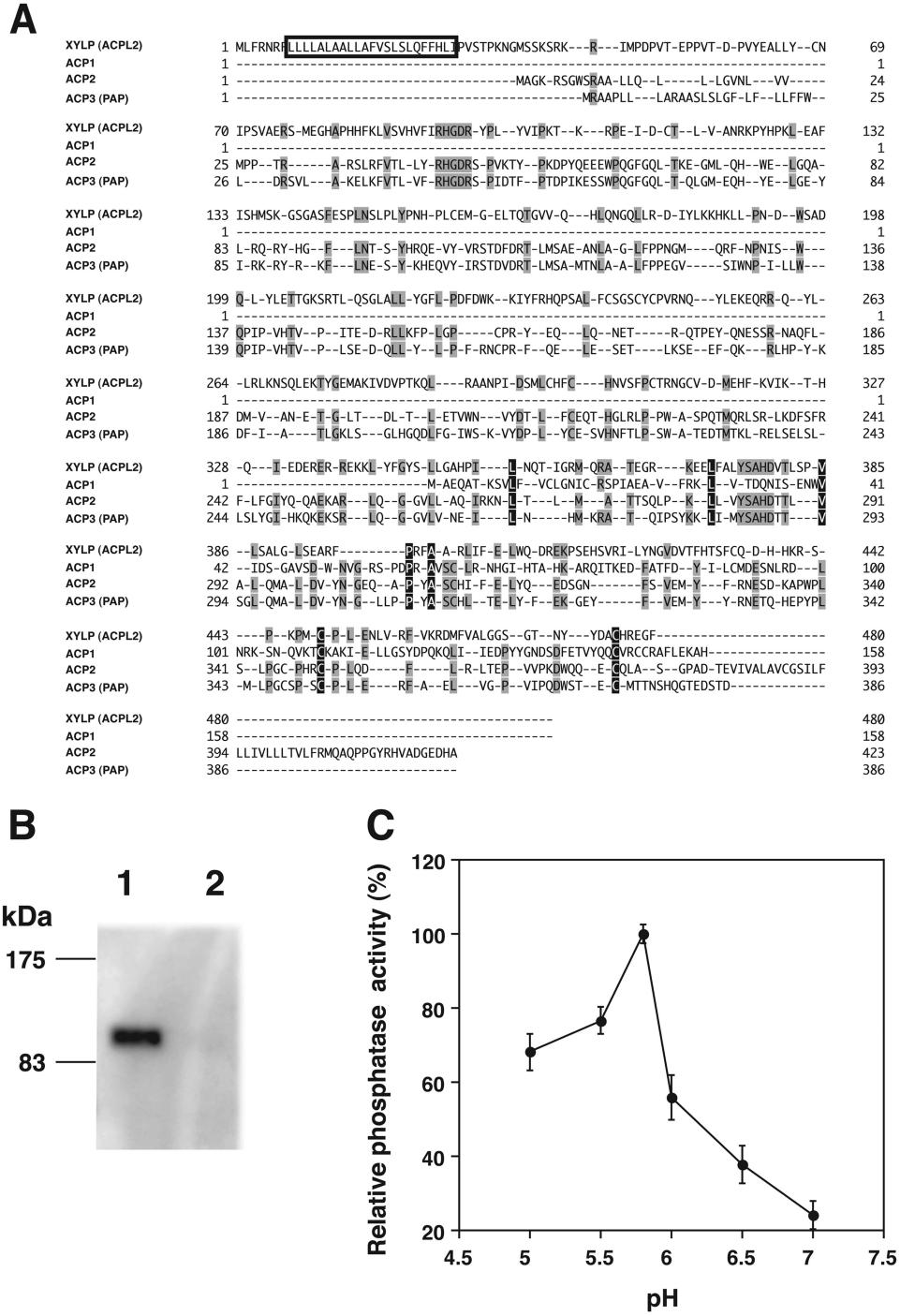

FIGURE 2. **Comparison of *XYLP* with other acidic phosphatase gene family members and charactrization of recombinant XYLP.** *A*, predicted amino acid sequences were aligned using the program GENETYX-MAC (version 13). *Closed* and *shaded boxes* indicate that the predicted amino acid in the alignment is identical in all four or any three, respectively, sequences. *Gaps* introduced for maximal alignment are indicated by *dashes*. The putative membrane spanning domains are *boxed*. *ACPL2,* acid phosphatase-like-2; *ACP,* acid phosphatase; *PAP,* prostate acid phosphatase. *B*, culture medium from cells transfected with XYLP expression construct or vector alone was incubated with IgG-Sepharose, and proteins purified from the medium were subjected to SDS-PAGE; expression of each protein A-tagged protein was examined with anti-mouse IgG antibody. *Lane 1*, XYLP-protein A; *lane 2*, vector alone. *C*, effects of pH on XYLP-catalyzed dephosphorylation of Gal-Gal-[^{32}P]Xyl(2-*O*-phosphate) were determined under standard assay conditions with different buffers. Data represent the average of three independent experiments.

(Golgi-DsRed) or an ER marker (ER-DsRed) in HeLa cells; we used confocal microscopy to examine the subcellular localization of the fluorescent proteins. XYLP-EGFP (Fig. 3*A*) co-localized with the Golgi-DsRed marker (Fig. 3*C*), but XYLP-EGFP (Fig. 3*D*) did not completely co-localize with the ER-DsRed marker (Fig. 3*F*). These results indicate that XYLP acted as a 2-phosphoxylose phosphatase in the Golgi apparatus.

Involvement of XYLP in GAG Biosynthesis—To further examine the physiological relevance of XYLP, we investigated whether overexpression of *XYLP* changes the amount of GAGs

TABLE 1
Comparison of substrate specificity of the phosphatases, XYLP and alkaline phosphatase (ALP)

Substrate[a]	XYLP[b]	ALP
	nmol/mg/h	
Gal-Gal-Xyl(2P)-TM	4.1 ± 0.4	4.8 ± 0.1
GlcUA-Gal-Gal-Xyl(2P)-TM	–[c]	4.9 ± 0.1
GalNAc-GlcUA-Gal-Gal-Xyl(2P)-TM	4.5 ± 0.5	4.8 ± 0.3
GlcNAc-GlcUA-Gal-Gal-Xyl(2P)-TM	–	4.4 ± 0.2
Osteopontin	–	1.0 ± 0.2
Matrix extracellular phosphoglycoprotein	–	0.2 ± 0.1

[a] 2P represents 2-*O*-phosphate.
[b] The values are the mean ± S.D. of three measurements.
[c] –, not detected (<0.1 nmol/mg/h).

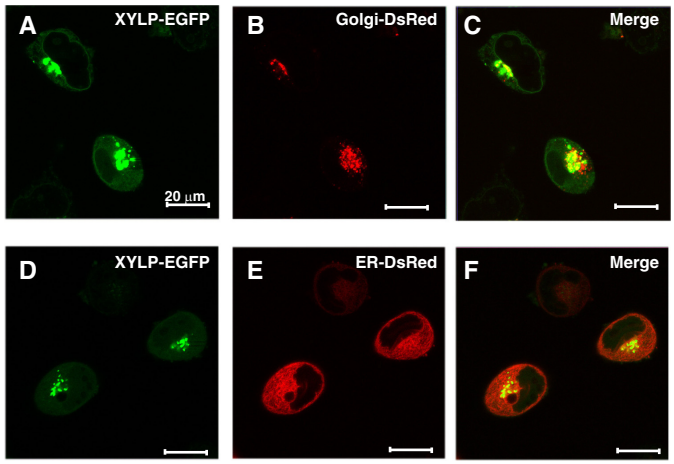

FIGURE 3. **Subcellular localization of XYLP.** Confocal microscopy was used to examine HeLa cells co-expressing XYLP-EGFP (*A*) and Golgi-DsRed (Golgi marker) (*B*) or co-expressing XYLP-EGFP (*D*) and ER-DsRed (ER marker) (*E*). The merged images show that XYLP precisely co-localized with a Golgi-DsRed marker (*C*) and that XYLP-EGFP was not completely co-localized with an ER-DsRed marker (*F*).

present in HeLa cells. As shown in Table 2, the composition of the disaccharides and the amount of CS and HS isolated from clones stably transfected with transgenic *XYLP* were determined by HPLC; these clones were designated *XYLP*-1 cells. The disaccharide composition of CS and of HS in the *XYLP*-1 cells was similar to that in the control HeLa cells; however, the total amount of CS and of HS was greater in *XYLP*-1 cells than in control cells. This augmentation was small probably because endogenous levels of *XYLP* are high in HeLa cells.

Thus, we examined whether knockdown of *XYLP* decreased the amount of CS and HS in HeLa cells. The efficiency of *XYLP* gene silencing was determined by quantitative real time RT-PCR. Transfection of shRNA *XYLP*-1 or shRNA *XYLP*-2 (two different shRNAs directed against *XYLP*) resulted in 83 or 87% knockdown, respectively, of *XYLP* mRNA. shRNA *XYLP*-1 and shRNA *XYLP*-2 resulted in a 33 or 54% decrease, respectively, in the amount of CS. Similarly, shRNA *XYLP*-1 and shRNA *XYLP*-2 resulted in a 27 or 47% decrease, respectively, in the amount of HS. In each assay, shRNA *XYLP*-1 cells or shRNA *XYLP*-2 cells were compared with shRNA control HeLa cells. Taken together, these results indicated that XYLP regulates the total amount of GAG synthesized in cells and plays an important role in the biosynthesis of GAGs.

Involvement of XLYP in the Increased Number of CS and HS Chains—We next compared the length and number of CS and HS chains obtained from the shRNA *XYLP*-2 with those obtained from shRNA control HeLa cells. Gel filtration analysis using a Superdex 200 column revealed that the length of the CS and HS chains in shRNA *XYLP*-2 cells was similar to that in the shRNA control cells; however, the number of short and long HS chains in *xylp*-2 cells was smaller than that in shRNA control cells (Fig. 4, *A* and *B*). These results indicated that XYLP might regulate the number of CS and HS chains.

Knockdown of XYLP Increased the Amount of Phosphorylated Linkage Structures—To further examine whether linkage region maturation was influenced by knockdown of *XYLP* in HeLa cells, the linkage oligosaccharides obtained from the shRNA *XYLP*-2 cells were compared with those obtained from shRNA cells. The 2-phosphoxylose in each cell line was radiolabeled with [^{32}P]NaH_2PO_4 and isolated after mild alkaline treatment with LiOH, which releases *O*-linked polysaccharides (including GAGs) from core proteins via β-elimination. The isolated oligosaccharides were derivatized with the fluorophore 2AB and separated by gel filtration chromatography using a Superdex peptide column; three predominant peaks were evident (Fig. 5*A*). The fraction 1 peak was larger in shRNA *xylp*-2 HeLa cells (Fig. 5*A*); therefore, fraction 1 was subjected to further analyses. The oligosaccharides in fraction 1 isolated from shRNA *XYLP*-2 HeLa cells were digested with heparitinase, which can cleave the α1–4 linkage of GlcNAcβ1–4GlcUA (20). Interestingly, these heparitinase-treated oligosaccharides shifted to the elution position of GlcUAβ1–3Galβ1–3Galβ1–4Xyl(2-*O*-phosphate)-2AB (Fig. 5*B*). In contrast, the oligosaccharides in fraction 1 were resistant to chondroitinase AC-II, which can cleave the β1–4 linkage of GalNAcβ1–4GlcUA, and to β-glucuronidase, which catalyzes hydrolysis of β-GlcUA residues from the nonreducing termini of sugar chains (Fig. 5*B*). As expected, the oligosaccharides in fraction 1 were sensitive to alkaline phosphatase, and they co-eluted with the authentic phosphorylated pentasaccharide GlcNAcα1–4GlcUAβ1–3Galβ1–3Galβ1–4Xyl(2-*O*-phosphate)-2AB (data not shown). Based on these findings, we concluded that the structure of the oligosaccharides in fraction 1 was GlcNAcα1–4GlcUAβ1–3Galβ1–3Galβ1–4Xyl(2-*O*-phosphate)-2AB. Notably, the amount of GlcNAcα1–4GlcUAβ1–3Galβ1–3Galβ1–4[^{32}P]Xyl(2-*O*-phosphate)-2AB was significantly lower in shRNA control cells than in *XYLP* knockdown or *FAM20B*-overexpressing cells; however, neither GalNAcα1–4GlcUAβ1–3Galβ1–3Galβ1–4[^{32}P]Xyl(2-*O*-phosphate)-2AB nor GlcUAβ1–3Galβ1–3Galβ1–4[^{32}P]Xyl(2-*O*-phosphate)-2AB was evident in any sample examined (Table 3). We recently demonstrated that GlcNAcα1–4GlcUAβ1–3Galβ1–3Galβ1–4[^{32}P]Xyl(2-*O*-phosphate) is formed by EXTL2 and considered to be a biosynthetic intermediate of an immature GAG chain (20). Therefore, when the formation of the phosphorylated linkage region is excessively accelerated by FAM20B or dephosphorylation by XYLP was attenuated, phosphorylated linkage tetrasaccharide could be formed; EXTL2 may then immediately transfer a GlcNAc to the phosphorylated linkage tetrasaccharide.

Furthermore, the oligosaccharides in fraction 2 eluted at the position of the authentic 2AB-trisaccharide Galβ1–3Galβ1–4[^{32}P]Xyl(2-*O*-phosphate)-2AB; similarly, the oligosaccharides in fraction 3 were eluted at the position of the authentic 2AB-disaccharide Galβ1–4[^{32}P]Xyl(2-*O*-phosphate)-2AB. The

TABLE 2

Disaccharide composition of GAGs from HeLa clones

HeLa cells were transfected with vector alone (mock) and plasmids containing *XYLP*, shRNA control, or shRNA *XYLP*. For experimental details, see "Experimental Procedures." The values are expressed as picomoles of disaccharide per mg of dried homogenate of these cells and as the means ± S.E. of three determinations.

	pmol/mg (mol%)				
CS Disaccharides	Mock	*XYLP*-1	shRNA-control	shRNA *XYLP*-1	shRNA *XYLP*-2
ΔHexA[a]-GalNAc	7.8 ± 1.0 (5)	10.1 ± 1.5 (6)	4.1 ± 1.4 (3)	3.4 ± 0.3 (4)	2.7 ± 1.0 (4)
ΔHexA-GalNAc(6S)	28.8 ± 5.1 (18)	46.6 ± 6.2 (28)	19.5 ± 0.5 (14)	14.6 ± 0.2 (16)	12.1 ± 0.3 (19)
ΔHexA-GalNAc(4S)	106.7 ± 8.7(68)	97.9 ± 12.8(59)	104.1 ± 2.1(75)	69.6 ± 1.9 (74)	45.2 ± 1.9 (71)
ΔHexA(2S)-GalNAc(6S)	8.3 ± 3.3 (5)	6.9 ± 0.8 (4)	6.3 ± 0.3 (4)	3.9 ± 0.1 (4)	2.3 ± 0.2 (4)
ΔHexA-GalNAc(4S,6S)	4.8 ± 1.6 (3)	3.7 ± 1.6 (2)	5.2 ± 0.1 (4)	2.2 ± 0.6 (2)	1.5 ± 0.6 (2)
ΔHexA(2S)-GalNAc(4S,6S)	__[c]	—	—	—	—
Total CS disaccharide	156.4 ± 19.4	165.2 ± 21.2	139.0 ± 10.2	93.7 ± 0.8	63.7 ± 2.7
HS Disaccharides	Mock	*XYLP*-1	shRNA-control	shRNA *XYLP*-1	shRNA *XYLP*-2
ΔHexA-GlcNAc	162.2 ± 18.9 (46)	162.8 ± 39.6 (43)	143.5 ± 10.9(41)	105.6 ± 3.9 (41)	83.0 ± 3.9 (45)
ΔHexA-GlcNAc(6S)	10.3 ± 0.9(3)	10.0 ± 3.5 (3)	9.4 ± 0.7(3)	6.6 ± 0.1 (3)	4.4 ± 1.0 (2)
ΔHexA-GlcN(NS)	123.8 ± 19.3 (35)	146.6 ± 36.8(39)	127.0 ± 10.2(37)	89.6 ± 3.3 (35)	65.2 ± 4.0 (35)
ΔHexA-GlcN(NS,6S)	12.2 ± 1.1 (3)	20.2 ± 5.2 (5)	14.7 ± 1.4(4)	9.0 ± 0.2 (4)	9.1 ± 0.8 (5)
ΔHexA(2S)-GlcN(NS)	25.1 ± 2.4 (7)	27.3 ± 9.7 (7)	29.6 ± 2.5(9)	23.4 ± 1.0 (9)	11.8 ± 1.9 (6)
ΔHexA(2S)-GlcN(NS,6S)	22.1 ± 1.6 (6)	24.6 ± 11.3(6)	24.1 ± 2.7(7)	21.6 ± 0.9 (8)	12.4 ± 2.0 (7)
Total HS disaccharide	355.8 ± 34.8	381.4 ± 84.8	348.3 ± 28.3	255.8 ± 9.2	185.8 ± 12.9
Relative expression[b]	1.0	2.7	1.0	0.17	0.13

[a] ΔHexA, GalNAc, GlcN, and GlcNAc represent unsaturated hexuronic acid, *N*-acetylgalactosamine, glucosamine, and *N*-acetylglucosamine, respectively; 6S, 4S, NS, and 2S represent 6-*O*-sulfate, 4-*O*-sulfate, 2-*N*-sulfate, and 2-*O*-sulfate, respectively.

[b] Quantitative real time RT-PCR was used to measure relative amounts of the *XYLP* transcript. *XYLP* mRNA levels were normalized relative to glyceraldehyde-3-phosphate dehydrogenase mRNA levels.

[c] —, not detected (<0.01 pmol/mg).

structural identity of these two oligosaccharides was further confirmed by co-chromatography using HPLC. The amounts of Galβ1–4[^{32}P]Xyl(2-*O*-phosphate)-2AB were significantly higher in *FAM20B*-overexpressing cells or in *XYLP* knockdown cells than in the shRNA control cells (Table 3). In addition, the amounts of Galβ1–3Galβ1–4[^{32}P]Xyl(2-*O*-phosphate)-2AB were greater in the samples from the *XYLP* knockdown cells than those from shRNA control cells. In contrast, the amounts of Galβ1–3Galβ1–4[^{32}P]Xyl(2-*O*-phosphate)-2AB were significantly lower in *FAM20B* knockdown cells than in control cells. All of these results closely correlated with *in vitro* XYLP and FAM20B substrate specificities. Interestingly, the phosphorylated linkage tetrasaccharide, GlcUAβ1–3Galβ1–3Galβ1–4[^{32}P]Xyl(2-*O*-phosphate)-2AB, was not detected in any sample examined; therefore, the addition of GlcUA may be accompanied by rapid dephosphorylation as proposed previously (11). Together, these results indicated that XYLP was a 2-phosphoxylose phosphatase that dephosphorylates Xyl residues in the GAG-protein linkage region in these HeLa cells.

Real Time PCR Analysis of XYLP in Several Human Tissues—Real time PCR and first strand cDNAs from different human tissues were used to assess the tissue-specific expression pattern of *XYLP* and *FAM20B*. Both enzymes were expressed ubiquitously, but somewhat differentially, in all tissues examined. The strong *XYLP* expression was evident in the spleen and fetal liver, and moderate expression was evident in the placenta, pancreas, kidney, thymus, and colon. Notably, the expression pattern was similar to that of *FAM20B* in the heart, pancreas, prostate, ovary, and small intestine and different from that of *FAM20B* in the placenta, lung, liver, kidney, spleen, thymus, colon, and fetal liver (Fig. 6).

Interactions of XYLP and GlcAT-I—To evaluate interactions between XLYP and GlcAT-I, co-expression of XLYP and GlcAT-I was carried out. First, to confirm that the co-expression of two proteins augments the dephosphorylation activity, the culture medium from each transfection experiment was incubated with IgG-Sepharose, and the IgG-Sepharose-bound proteins were then evaluated for enzyme activity. Dephosphorylation activity was evident in medium from each transfectant when Gal-Gal-[^{32}P]Xyl(2-*O*-phosphate)-TM was used as a substrate (Table 4). Remarkably, in the presence of UDP-GlcUA, co-expression of XYLP and GlcAT-I augmented the dephosphorylation activity of XYLP over 16-fold (Table 4), although such an augmentation was not observed in the absence of UDP-GlcUA. These results suggest that the addition of the first GlcUA residue by GlcAT-I was accompanied by rapid dephosphorylation by XYLP. Then, to clarify the involvement of the transfer of GlcUA in a marked augmentation of the dephosphorylation activity, we constructed a GlcAT-I mutant, which is expected to lack GlcAT-I activity. Based on the crystal structure of GlcAT-I, the residue Glu-281 is in position to function as a catalytic base (29, 30). In fact, the GlcAT-I E281A mutant

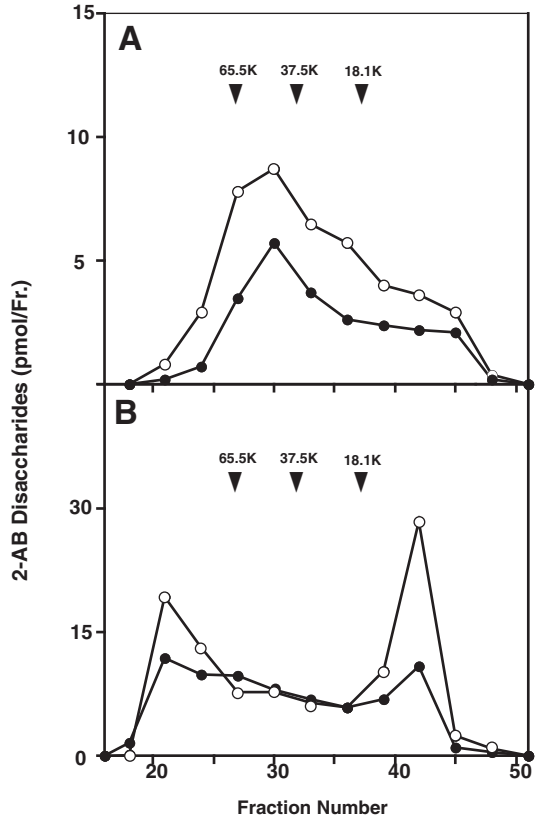

FIGURE 4. **Analysis of the lengths of CS and HS chains from HeLa-shRNA control and HeLa-shRNA *XYLP*-2 cells.** Purified GAG fractions were subjected to reductive β-elimination with $NaBH_4$/NaOH and then analyzed by gel filtration chromatography on a Superdex 200 column (10 × 300 mm). The digests of individual fractions obtained with chondroitinase ABC (*A*) or a mixture of heparinase and heparitinase (*B*) were derivatized with 2AB and then analyzed by HPLC. The amounts of the 2AB derivatives of unsaturated disaccharides were calculated based on fluorescence intensity. Data from samples from shRNA *XYLP*-2 (●) and shRNA control HeLa cells (○) are shown. The *arrowheads* labeled *65.5K*, *37.5K*, and *18.1K* indicate the elution position of the 65.5-, 37.5-, and 18.1-kDa saccharides, respectively; these molecular weight determinations were based on the elution positions of commercial polysaccharides of known sizes (dextran average M_r: 65,500; 37,500; and 18,100; all from Sigma). Data represent 1 of 3 independent series of experiments, where all three series gave essentially identical results.

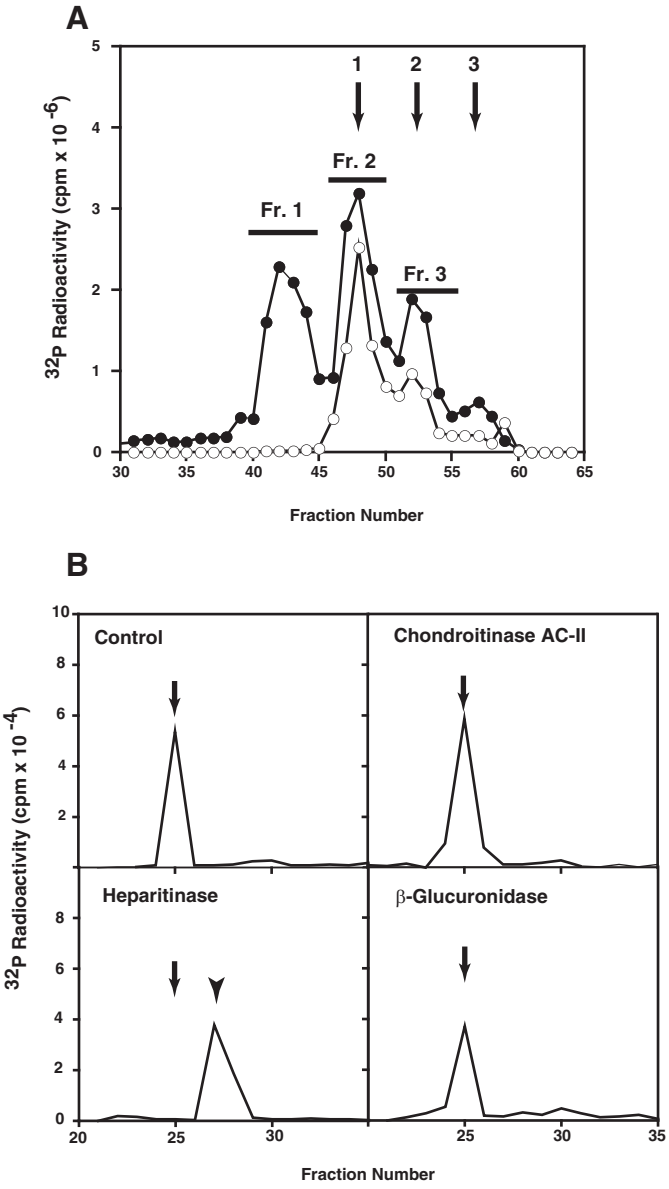

FIGURE 5. **Characterization of the linkage oligosaccharides isolated from HeLa cells.** *A*, 2AB-labeled oligosaccharides were separated by gel filtration on Superdex peptide columns. The *arrows* denote the elution positions of the following compounds: *1*, Galβ1–3Galβ1–4Xyl(2-*O*-phosphate)-2AB; *2*, Galβ1–4Xyl(2-*O*-phosphate)-2AB; *3*, free [^{32}P]phosphate. Data from samples from shRNA *XYLP*-2 (●) and shRNA control HeLa cells (○) are shown. *Fr., fraction*. *B*, oligosaccharides in pooled fraction 1 were digested with various glycosidases, and digests were analyzed by HPLC on a column of PA-03. The *arrows* and the *arrowheads* denote the elution positions of the authentic compounds, GlcNAcα1–4GlcUAβ1–3Galβ1–3Galβ1–4Xyl(2-*O*-phosphate)-2AB and GlcUAβ1–3Galβ1–3Galβ1–4Xyl(2-*O*-phosphate)-2AB, respectively.

would not possess GlcAT-I activity. Notably, co-expression of XYLP and the GlcAT-I E281A mutant did not result in a marked augmentation of the dephosphorylation activity even in the presence of UDP-GlcUA.

Next, we used pulldown assays to determine whether interactions between XYLP and GlcAT-I occurred. For this analysis, soluble forms of protein A-tagged XYLP fusion proteins (XYLP-ProA) and a soluble form of a His_6-tagged GlcAT-I, GalT-II, and Fam20B fusion protein (GlcAT-I-His, GalT-II-His, and Fam20B-His, respectively) were generated. To evaluate associations among these proteins, pulldown assays were performed. In addition, to ensure specificity, we conducted these assays with GalT-II or FAM20B (a Xyl kinase). For this analysis, soluble forms of a protein A-tagged XYLP fusion protein (XYLP-ProA) and His_6-tagged GlcAT-I, GalT-II, and Fam20B fusion proteins (GlcAT-I-His, GalT-II-His, and Fam20B-His, respectively) were generated. Ni-NTA-agarose was added to the culture medium to pull down His-tagged proteins. Then, the proteins were subjected to SDS-PAGE followed by Western blotting, and the resulting blots were probed with IgG antibody; antibody signal was detected with an ECL select detection reagent. No band was detected with samples from the co-transfectant expressing XYLP-ProA and GalT-II-His or XYLP-ProA and Fam20B-His (Fig. 7*A*). However, proteins with a molecular mass of ~90 kDa and corresponding to XYLP-ProA were detected with samples from the co-transfectant expressing XYLP-ProA and GlcAT-I-His (Fig. 7*A*).

Then, to investigate the intracellular localization of XYLP in the presence or absence of GlcAT-I, XYLP-EGFP was co-ex-

TABLE 3

Proportion of phosphorylated linkage-region saccharides from HeLa clones

HeLa cells were transfected with plasmids containing *FAM20B*, shRNA control, shRNA *XYLP*, or shRNA *FAM20B*. ^{32}P radioactivity was measured as described under "Experimental Procedures."

Structure	shRNA control	shRNA XYLP-2	FAM20B	shRNA FAM20B
Gal-[^{32}P]Xyl(2P)-2AB[a]	1.0 ± 0.15[b]	1.72 ± 0.12[c]	3.12 ± 0.29[c]	0.97 ± 0.05
Gal-Gal-[^{32}P]Xyl(2P)-2AB	3.4 ± 1.38	5.75 ± 1.19	2.32 ± 0.17	0.86 ± 0.06[c]
GlcUA-Gal-Gal-[^{32}P]Xyl(2P)-2AB	–[d]	–	–	–
GalNAc-GlcUA-Gal-Gal-[^{32}P]Xyl(2P)-2AB	–	–	–	–
GlcNAc-GlcUA-Gal-Gal-[^{32}P]Xyl(2P)-2AB	0.08 ± 0.04	3.58 ± 0.19[e]	0.39 ± 0.03[c]	0.08 ± 0.02

[a] 2P represents 2-*O*-phosphate.
[b] The values of Gal-Xyl(2P)-2AB derived from shRNA control cells were set at a value of 1.0. The values are the means ± S.E. of three determinations.
[c] $p < 0.05$; the values of Gal-Xyl(2P)-2AB were derived from shRNA control cells *versus* from shRNA *XYLP*-2 cells; the values of Gal-Xyl(2P)-2AB were derived from shRNA control cells *versus* from *FAM20B*-overexpressing cells; the values of Gal-Gal-Xyl(2P)-2AB were derived from shRNA control cells *versus* from shRNA *FAM20B* cells, and the values of GlcNAc-GlcUA-Gal-Gal-Xyl(2P)-2AB were derived from shRNA control cells *versus* from *FAM20B*-overexpressing cells.
[d] $p < 0.001$; the values of GlcNAc-GlcUA-Gal-Gal-Xyl(2P)-2AB were derived from shRNA control cells *versus* from shRNA *XYLP*-2 cells.
[e] –, not detected (<0.01).

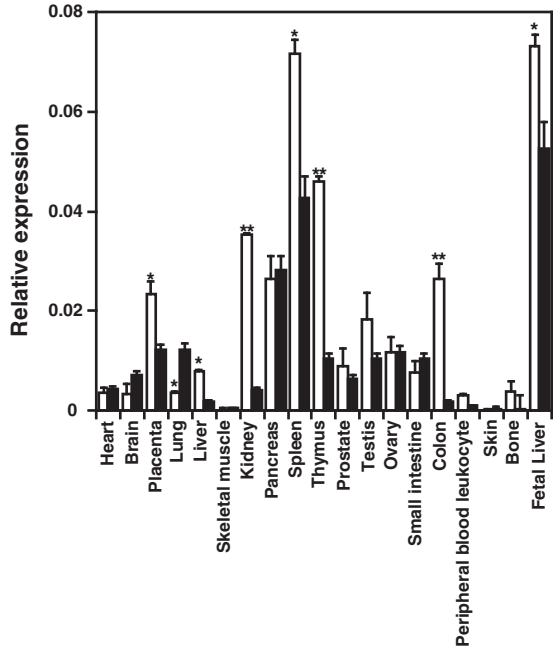

FIGURE 6. **Expression levels of *XYLP* mRNA in different human tissues.** Multiple tissue cDNA panels (Clontech) were used to perform real time PCR analyses. Levels of *XYLP* (*open bars*) and *FAM20B* (*closed bars*) mRNAs were normalized to those of glyceraldehyde-3-phosphate dehydrogenase mRNA. Results are means ± S.E. of three experiments. Statistical analysis was carried out by Student's *t* test. *, $p < 0.01$, and **, $p < 0.05$.

TABLE 4

Comparison of phosphatase activities of XYLP and co-transfectant of XYLP and GlcAT-I

Substrate[a]	XYLP[b]	XYLP/ GlcAT-I
	nmol/mg/h	
Gal-Gal-Xyl(2P)-TM	4.1 ± 0.4	3.3 ± 1.1
Gal-Gal-Xyl(2P)-TM + UDP-GlcUA	1.7 ± 0.5	27.7 ± 5.3
GlcUA-Gal-Gal-Xyl(2P)-TM	–[c]	–
GlcUA-Gal-Gal-Xyl(2P)-TM+ UDP-GlcUA	–	–

[a] 2P represents 2-*O*-phosphate.
[b] The values are the mean ± S.D. of three measurements.
[c] –, not detected (<0.1 nmol/mg/h).

pressed with a Golgi-DsRed or an ER-DsRed in wild-type or *GlcAT-I*$^{-/-}$ ESCs (21), respectively. In the presence of GlcAT-I (wild-type ESCs), XYLP-EGFP co-localized with the Golgi-DsRed marker, but XYLP-EGFP did not completely co-localize with the ER-DsRed marker (Fig. 7, *B* and *C*). These results were consistent with those obtained in HeLa cells (see Fig. 3, *A* and *C*). Remarkably, in the absence of GlcAT-I (*GlcAT-I*$^{-/-}$ ESCs), XYLP-EGFP co-localized predominantly with the ER-DsRed marker, whereas XYLP-EGFP did not completely co-localize with the Golgi-DsRed marker (Fig. 7, *B* and *C*). These results indicate that XYLP is transported to the Golgi with interaction of GlcAT-I and that expression of GlcAT-I is indispensable for accumulation of XYLP in the Golgi complex.

To further examine whether XYLP-dependent dephosphorylation is influenced by knock-out of GlcAT-I, the linkage oligosaccharides obtained from the *GlcAT-I*$^{-/-}$ ESCs were compared with those obtained from wild-type ESCs. The 2-phosphoxylose in each cell line was radiolabeled with [^{32}P]NaH_2PO_4 and isolated after mild alkaline treatment with LiOH as described above. The isolated oligosaccharides were derivatized with the fluorophore 2AB and separated by gel filtration chromatography using a Superdex peptide column. As expected, GlcUAβ1–3Galβ1–3Galβ1–4[^{32}P]Xyl(2-*O*-phosphate)-2AB, GalNAcα1–4GlcUAβ1–3Galβ1–3-Galβ1–4[^{32}P]Xyl(2-*O*-phosphate)-2AB, and GlcNAcα1–4-GlcUAβ1–3Galβ1–3Galβ1–4[^{32}P]Xyl(2-*O*-phosphate)-2AB were not detected. Notably, the amounts of Galβ1–3 Galβ1–4[^{32}P]Xyl(2-*O*-phosphate)-2AB and Galβ1–4[^{32}P]X-yl(2-*O*-phosphate)-2AB were significantly higher in *GlcAT-I*$^{-/-}$ than wild-type ESCs (Table 5), despite the fact that XYLP was expressed in both wild-type and *GlcAT-I*$^{-/-}$ ESCs. These results also suggest that GlcAT-I-mediated addition of GlcUA might facilitate the XYLP-dependent dephosphorylation. Taken together, these results indicated that XYLP and GlcAT-I interacted with each other and that GlcAT-I-mediated addition of GlcUA can be accompanied by rapid XYLP-dependent dephosphorylation during completion of linkage region formation.

DISCUSSION

Previously, we demonstrated that FAM20B is a Xyl kinase that phosphorylates C2 of the Xyl residue in the GAG-protein linkage region of nonphosphorylated trisaccharide serine structures (Galβ1–3Galβ1–4Xylβ1-*O*-Ser) (14). Additionally, Moses *et al.* (11, 12) demonstrated that phosphorylation gradually increases as the linkage region forms and that Xyl phosphorylation was completed at the Galβ1–3Galβ1–4Xyl stage. Only the trisaccharide contained an almost fully phosphorylated Xyl. Addition of the first GlcUA residue was accompanied by rapid dephosphorylation, suggesting that the phosphoryla-

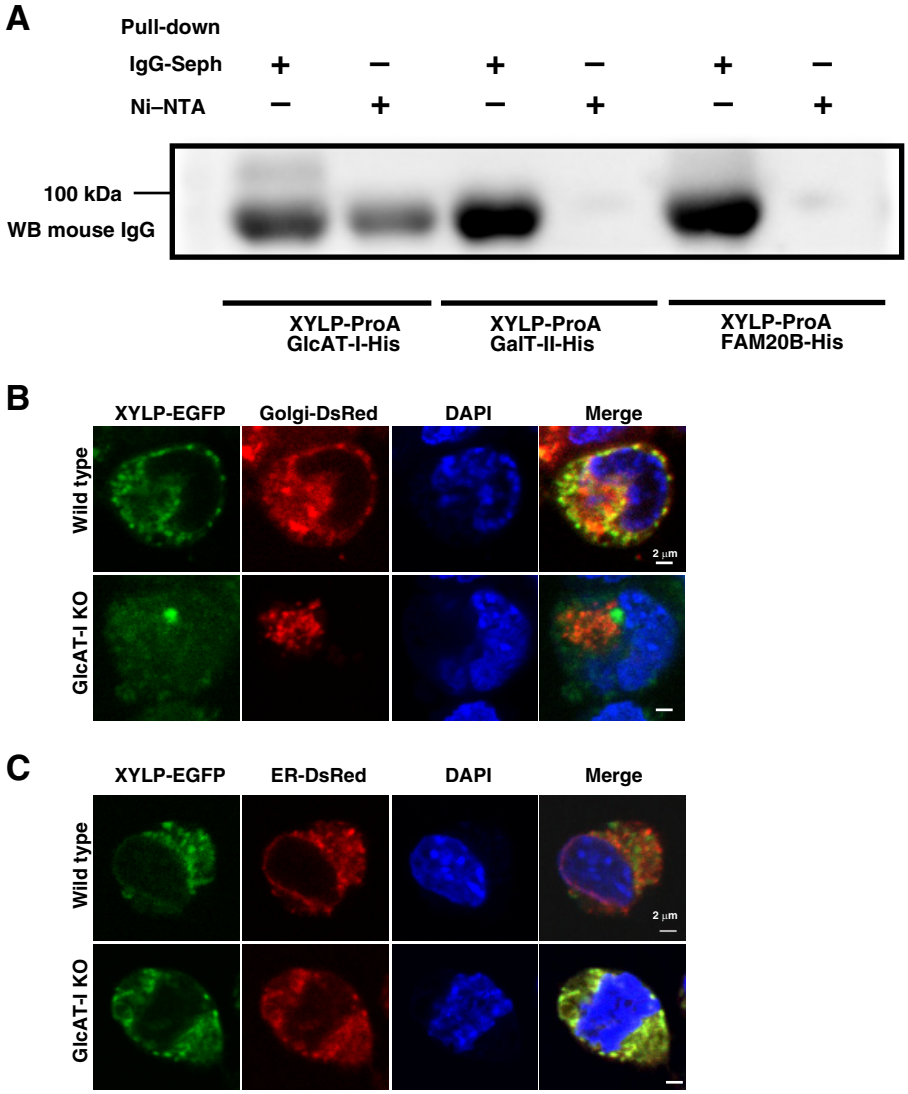

FIGURE 7. **Interactions of XYLP and GlcAT-I.** *A,* culture medium from cells co-expressing XYLP-ProA and GlcAT-I-His, XYLP-ProA and GalT-II-His, or XYLP-ProA and FAM20B-His was incubated with Ni-NTA-agarose to purify His_6-tagged proteins and any associated proteins; the purified proteins were subjected to SDS-PAGE. The separated proteins were transferred to PVDF membrane and allowed to react with IgG as a primary antibody; ECL select detection reagent was used to visualize antibody-labeled proteins. *B* and *C,* XYLP-EGFP was co-expressed with a Golgi-DsRed (*B*) or an ER-DsRed (*C*) in wild-type or *GlcAT-I*$^{-/-}$ ESCs, respectively. *B,* XYLP-EGFP co-localized with the Golgi-DsRed marker in wild-type ESCs, but XYLP-EGFP did not completely co-localize with the Golgi-DsRed marker in *GlcAT-I*$^{-/-}$ ESCs. *C,* XYLP-EGFP did not completely co-localize with the ER-DsRed marker in wild-type ESCs, but XYLP-EGFP co-localized with the ER-DsRed marker in *GlcAT-I*$^{-/-}$ ESCs. *Seph,* Sepharose; *WB,* Western blot.

TABLE 5

Proportion of phosphorylated linkage-region saccharides from ESCs

Wild-type and *GlcAT-I*$^{-/-}$ ESCs were isolated from the inner cell mass of explanted blastocysts derived from heterozygous intercrosses (*GlcAT-I*$^{+/-}$ × *GlcAT-I*$^{+/-}$) (21). ^{32}P radioactivity was measured as described under "Experimental Procedures."

Structure	Wild-type ESCs	*GlcAT-I*$^{-/-}$ ESCs
Gal-[^{32}P]Xyl(2P)-2AB[a]	1.0 ± 0.2[b]	2.0 ± 0.2[c]
Gal-Gal-[^{32}P]Xyl(2P)-2AB	2.14 ± 0.32	3.37 ± 0.27[c]
GlcUA-Gal-Gal-[^{32}P]Xyl(2P)-2AB	–[d]	–
GalNAc-GlcUA-Gal-Gal-[^{32}P]Xyl(2P)-2AB	–	–
GlcNAc-GlcUA-Gal-Gal-[^{32}P]Xyl(2P)-2AB	5.83 ± 0.5	–

[a] 2P represents 2-*O*-phosphate.
[b] The values of Gal-Xyl(2P)-2AB derived from wild-type ESCs were set at a value of 1.0. The values are the means ± S.E. of three determinations.
[c] $p < 0.05$; the values of Gal-Xyl(2P)-2AB were derived from wild-type ESCs *versus* from *GlcAT-I*$^{-/-}$ ESCs, and the values of Gal-Gal-Xyl(2P)-2AB were derived from wild-type ESCs *versus* from *GlcAT-I*$^{-/-}$ ESCs.
[d] –, not detected (<0.01).

tion of Xyl is a transient phenomenon (11, 12). Thus, it is suggested that GlcAT-I-mediated addition of GlcUA can be accompanied by rapid XYLP-dependent dephosphorylation during completion of linkage region formation. In fact, the phosphorylated linkage tetrasaccharide was not detected in cells (Tables 3 and 5). In addition, XYLP and GlcAT-I can form heterooligomers apparently required for maximal dephosphorylation activity (Table 4) and translocation to the Golgi *in vitro* (Fig. 7, *B* and *C*). These findings are similar to those in the case of co-transfection of EXT1 and EXT2, which forms an enzyme complex for the polymerization of HS (31). In view of these results, both XYLP and GlcAT-I seem to be indispensable for efficient maturation of the linkage region tetrasaccharide. Thus, we concluded that the phosphorylation and dephosphorylation of Xyl residues were tightly regulated by FAM20B, XYLP, and GlcAT-I.

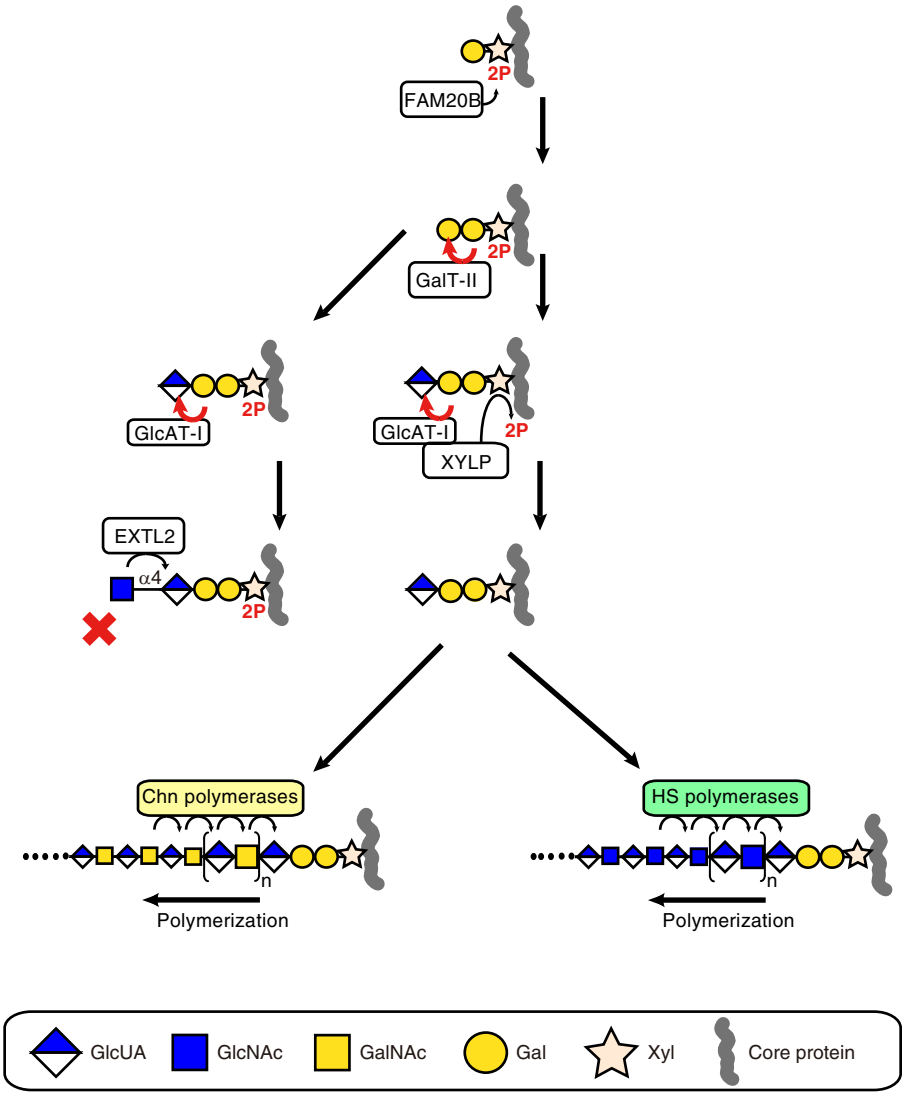

FIGURE 8. **Phosphorylation and dephosphorylation of Xyl residues regulate the formation of the linkage region and GAG biosynthesis.** Synthesis of the linkage region is initiated by the addition of a Xyl residue to a specific serine residue on a core protein; this event is followed by the sequential transfer of two Gal residues, and synthesis of the linkage region is completed by transfer of a GlcUA residue. During synthesis of the linkage region, transient FAM20B-catalyzed phosphorylation of the Xyl residue occurs and enhances the activity of GalT-II and of GlcAT-I. After synthesis of the phosphorylated linkage region trisaccharide, GlcAT-I transfers GlcUA to the phosphorylated trisaccharide serine structure, Galβ1–3Galβ1–4Xyl(2-*O*-phosphate)β1-*O*-Ser. Concomitant with this process, dephosphorylation of Xyl is immediately induced by XLYP. Then, chondroitin (*Chn*) or HS polymerases induce polymerization of disaccharide chains onto the linkage region tetrasaccharide. If formation of linkage region is excessively accelerated by FAM20B and/or dephosphorylation of the Xyl by XYLP is attenuated, biosynthetic intermediates (phosphorylated linkage tetrasaccharides) could accumulate; under this condition, EXTL2 may immediately transfer a GlcNAc to the phosphorylated linkage tetrasaccharide and thereby induce chain termination (20). *2P* represents 2-*O*-phosphate.

Here, we found that RNA interference of *XYLP* resulted in a reduction in the amounts of CS and HS in cells. In addition, gel filtration analysis of the GAG chains synthesized in the knockdown cells revealed that the CS and HS chains had similar lengths to CS and HS chains, respectively, in shRNA control cells. These results indicated that XYLP regulated the number of CS and HS chains. These findings are in agreement with the results that the phosphorylated linkage tetrasaccharide did not serve as a substrate for chondroitin or HS polymerization. Therefore, we reasoned that dephosphorylation of the Xyl residue by XYLP may be required for biosynthetic maturation of the linkage region sequence and that this maturation may be a prerequisite for the initiation and the efficient elongation of the repeating disaccharide region of GAG chains. Similarly, overexpression of *FAM20B* increased the amount of both CS and HS in HeLa cells, and RNA interference of *FAM20B* resulted in a reduction in the amounts of both CS and HS in the cells (14). Gel filtration analysis of the GAG chains synthesized in cells that overexpressed *FAM20B* revealed that they had lengths similar to those in the mock-transfected cells (14). These results also indicate that FAM20B regulates the number of GAG chains by phosphorylating the Xyl residue in the GAG-protein linkage region of proteoglycans. In this regard, it should be noted that GlcAT-I could efficiently transfer a GlcUA residue to the phosphorylated trisaccharide serine, Galβ1–3Galβ1–4Xyl(2-*O*-phosphate)β1-*O*-Ser, than to the nonphosphorylated counterpart Galβ1–3Galβ1–4Xylβ1-*O*-Ser (10). Moreover, in rat articular cartilage explants, the introduction of *GlcAT-I* enhanced GAG synthesis via an increase in the abundance rather than the length of GAG chains, whereas antisense

inhibition of *GlcAT-I* expression impaired GAG synthesis (32). These results suggest that GlcAT-I regulates the expression of GAGs in a Xyl phosphorylation-dependent manner. Therefore, we reasoned that phosphorylation and dephosphorylation of Xyl are coupled and that together these events regulate the number of GAG chains and play an important role in the biosynthesis of GAGs.

GAG chains exert their specific functions in a tissue- and cell type-specific manner, suggesting that the structure and amount of GAG chains are strictly regulated. A recent report suggested that abnormal biosynthesis of GAGs due to lack of EXTL2 affects liver injury, liver regeneration processes (33), and the progression of vascular calcification in cases of chronic kidney disease (34). *EXTL2* is one of three *EXT*-like genes homologous to the tumor suppressor *EXT* gene family members and encodes an *N*-acetylhexosaminyltransferase (20, 35). EXTL2 terminated polymerization of GAG chains by transferring an *N*-acetylglucosamine residue to the phosphorylated tetrasaccharide linkage region. Remarkably, the phosphorylated linkage pentasaccharide, GlcNAcβ1–4GlcUAβ1–3Galβ1–3-Galβ1–4Xyl(2-*O*-phosphate), was not used as an acceptor for HS or chondroitin polymerases. Furthermore, our previous study raised the possibility that the dephosphorylated linkage pentasaccharide, GlcNAcβ1–4GlcUAβ1–3Galβ1–3 Galβ1–4Xyl, is utilized as a primer for HS biosynthesis (20). These results suggest that persistent xylose phosphorylation of the pentasaccharide may prevent further polymerization of HS. If chain polymerization takes place at a slow rate despite accelerated formation of the linkage region (*e.g.* under pathological conditions and embryo development), the synthesis of a linkage region will be uncoupled from subsequent polymerization. In this situation, it is thought that XYLP functions as a regulator to control GAG biosynthesis. Unless the dephosphorylation-dependent regulation system operates, an increase in supply of phosphorylated tetrasaccharide linkage would cause a chain termination. In addition, *FAM20B*$^{-/-}$ mice have been reported to die as embryos and show severely stunted growth, multisystem organ hypoplasia, and delayed development of the skeletal system, eyes, lung, gastrointestinal tract, and liver (28). Based on these findings, we propose that both steps, the phosphorylation and dephosphorylation of a Xyl residue, are important for the maintenance of tissue homeostasis under pathological conditions and embryo development.

Here, we propose that the formation of GAG-protein linkage region is controlled via two pathways (Fig. 8). The biosynthesis of GAG is initiated by the addition of Xyl to specific serine residues in a core protein; this event is followed by the transfer of Gal residues and then by the transient phosphorylation of Xyl residues by FAM20B (14). Next, GlcAT-I transfers GlcUA from UDP-GlcUA to the phosphorylated trisaccharide serine structure, Galβ1–3Galβ1–4Xyl(2-*O*-phosphate)β1-*O*-Ser; this final step completes formation of the linkage region. Concomitantly, XYLP can dephosphorylate Xyl(2-*O*-phosphate)β1-*O*-Ser structures during this last step, and interactions between GlcAT-I and XYLP facilitate these two simultaneous steps. Then, CS or HS polymerization onto the linkage region tetrasaccharide can proceed via chondroitin or HS polymerases, respectively. In this model, phosphorylation of Xyl residues function to regulate linkage region synthesis, which is enhanced by GlcAT-I, and the dephosphorylation of Xyl residues facilitates the initiation of polymerization. Indeed, polymerization of the disaccharide repeats of GAG chains is initiated on dephosphorylated tetrasaccharide linkage structures (Fig. 1) (20). If the formation of the linkage region is excessively accelerated by FAM20B and/or the dephosphorylation of linkage region by XYLP is attenuated, biosynthetic intermediates (phosphorylated linkage tetrasaccharide) may accumulate; under this condition, EXTL2 immediately transfers a GlcNAc to the phosphorylated linkage tetrasaccharide and thereby induces chain termination (20). Whether the phosphorylated linkage pentasaccharide produced by EXTL2 can be recycled for HS biosynthesis and/or be degraded remains unclear. However, XYLP could not use the phosphorylated linkage pentasaccharide as a substrate (see Table 1); therefore, it is likely that this pentasaccharide will be degraded.

In conclusion, we identified the 2-phosphoxylose phosphatase responsible for the dephosphorylation of Xyl in the GAG-protein linkage region and found that transient phosphorylation of Xyl residues plays an important role in controlling the formation of GAG chains. Presumably, all encoding enzymes responsible for GAG biosynthesis in human cells have now been identified. Analyses, both *in vitro* and *in vivo*, of enzymatic and biological functions of the individual enzymes have provided novel insights into the existence of high order molecular complexes that produce structurally and functionally diverse GAG chains (1, 35). Therefore, a comprehensive assessment of physical and functional interactions among the individual enzymes, together with examination of the regulation their transcription and translation, will help to elucidate the biosynthetic fine-tuning of the various biological/pathological functions of GAG chains.

REFERENCES

1. Mikami, T., and Kitagawa, H. (2013) Biosynthesis and function of chondroitin sulfate. *Biochim. Biophys. Acta* **1830,** 4719–4733
2. Kitagawa, H., Uyama, T., and Sugahara, K. (2001) Molecular cloning and expression of a human chondroitin synthase. *J. Biol. Chem.* **276,** 38721–38726
3. Izumikawa, T., Uyama, T., Okuura, Y., Sugahara, K., and Kitagawa, H. (2007) Involvement of chondroitin sulfate synthase-3 (chondroitin synthase-2) in chondroitin polymerization through its interaction with chondroitin synthase-1 or chondroitin polymerizing factor. *Biochem. J.* **403,** 545–552
4. Izumikawa, T., Koike, T., Shiozawa, S., Sugahara, K., Tamura, J., and Kitagawa, H. (2008) Identification of chondroitin sulfate glucuronyltransferase as chondroitin synthase-3 involved in chondroitin polymerization: Chondroitin polymerization is achieved by multiple enzyme complexes consisting of chondroitin synthase family members. *J. Biol. Chem.* **283,** 11396–11406
5. Kitagawa, H., Izumikawa, T., Uyama, T., and Sugahara, K. (2003) Molecular cloning of a chondroitin polymerizing factor that cooperates with chondroitin synthase for chondroitin polymerization. *J. Biol. Chem.* **278,** 23666–23671
6. Mizumoto, S., Uyama, T., Mikami, T., Kitagawa, H., and Sugahara, K. (2005) in *Handbook of Carbohydrate Engineering* (Kevin J. Yarema, ed) pp. 289–324, CRC Press (Taylor & Francis Group), Boca Raton, FL
7. Oegema, T. R., Jr., Kraft, E. L., Jourdian, G. W., and Van Valen, T. R. (1984) Phosphorylation of chondroitin sulfate in proteoglycans from the swarm rat chondrosarcoma. *J. Biol. Chem.* **259,** 1720–1726
8. Fransson, L.-A, Silverberg, I., and Carlstedt, I. (1985) Structure of the heparan

sulfate-protein linkage region. Demonstration of the sequence galactosyl-galactosyl-xylose-2-phosphate. *J. Biol. Chem.* **260,** 14722–14726
9. Gulberti, S., Lattard, V., Fondeur, M., Jacquinet, J. C., Mulliert, G., Netter, P., Magdalou, J., Ouzzine, M., and Fournel-Gigleux, S. (2005) Phosphorylation and sulfation of oligosaccharide substrates critically influence the activity of human β1,4-galactosyltransferase 7 (GalT-I) and β1,3-glucuronosyltransferase I (GlcAT-I) involved in the biosynthesis of the glycosaminoglycan-protein linkage region of proteoglycans. *J. Biol. Chem.* **280,** 1417–1425
10. Tone, Y., Pedersen, L. C., Yamamoto, T., Izumikawa, T., Kitagawa, H., Nishihara, J., Tamura, J., Negishi, M., and Sugahara, K. (2008) 2-*O*-Phosphorylation of xylose and 6-*O*-sulfation of galactose in the protein linkage region of glycosaminoglycans influence the glucuronyltransferase-I activity involved in the linkage regions synthesis. *J. Biol. Chem.* **283,** 16801–16807
11. Moses, J., Oldberg, A., Cheng, F., and Fransson, L.-A. (1997) Biosynthesis of the proteoglycan decorin-transient 2-phosphorylation of xylose during formation of the trisaccharide linkage region. *Eur. J. Biochem.* **248,** 521–526
12. Moses, J., Oldberg, A., and Fransson, L.-A. (1999) Initiation of galactosaminoglycan biosynthesis. Separate galactosylation and dephosphorylation pathways for phosphoxylosylated decorin protein and exogenous xyloside. *Eur. J. Biochem.* **260,** 879 – 884
13. Fransson, L. A., Belting, M., Jönsson, M., Mani, K., Moses, J., and Oldberg, A. (2000) Biosynthesis of decorin and glypican. *Matrix Biol.* **19,** 367–376
14. Koike, T., Izumikawa, T., Tamura, J., and Kitagawa, H. (2009) FAM20B is a kinase that phosphorylates xylose in the glycosaminoglycan-protein linkage region. *Biochem. J.* **421,** 157–162
15. Eames, B. F., Yan, Y.-L., Swartz, M. E., Levic, D. S., Knapik, E. W., Postlethwait, J. H., and Kimmel C. B. (2011) Mutations in *fam20b* and *xylt1* revealed that cartilage matrix controls timing of endochondral ossification by inhibiting chondrocyte maturation. *PLoS Genet.* **7,** e1002246
16. Kim, B.-T., Kitagawa, H., Tanaka, J., Tamura, J., and Sugahara, K. (2003) *In vitro* heparan sulfate polymerization: Crucial roles of core protein moieties of primer substrates in addition to the EXT1-EXT2 interaction. *J. Biol. Chem.* **278,** 41618 – 41623
17. Nadanaka, S., Kitagawa, H., and Sugahara, K. (1998) Demonstration of the immature glycosaminoglycan tetrasaccharide sequence GlcAβ1–3Galβ1–3 Galβ1– 4Xyl on recombinant soluble human α-thrombomodulin: A possible mechanism generating "part-time" proteoglycans. *J. Biol. Chem.* **273,** 33728 –33734
18. Kitagawa, H., and Paulson, J. C. (1994) Cloning of a novel α2,3-sialyltransferase that sialylates glycoprotein and glycolipid carbohydrate groups. *J. Biol. Chem.* **269,** 1394 –1401
19. Uyama, T., Kitagawa, H., Tamura Ji J., and Sugahara, K. (2002) Molecular cloning and expression of human chondroitin *N*-acetylgalactosaminyltransferase: the key enzyme for chain initiation and elongation of chondroitin/dermatan sulfate on the protein linkage region tetrasaccharide shared by heparin/heparan sulfate. *J. Biol. Chem.* **277,** 8841– 8846
20. Nadanaka, S., Zhou, S., Kagiyama, S., Shoji, N., Sugahara, K., Sugihara, K., Asano, M., and Kitagawa, H. (2013) EXTL2, a member of the EXT family of tumor suppressors, controls glycosaminoglycan biosynthesis in a xylose kinase-dependent manner. *J. Biol. Chem.* **288,** 9321–9333
21. Izumikawa, T., Sato, B., and Kitagawa, H. (2014) Chondroitin sulfate is indispensable for pluripotency and differentiation of mouse embryonic stem cells. *Sci. Rep.* **4,** 3701; 10.1038/srep03701
22. Kinoshita, A., and Sugahara, K. (1999) Microanalysis of glycosaminoglycan-derived oligosaccharides labeled with a fluorophore 2-aminobenzamide by high-performance liquid chromatography: application to disaccharide composition analysis and exosequencing of oligosaccharides. *Anal. Biochem.* **269,** 367–378
23. Izumikawa, T., Okuura, Y., Koike, T., Sakoda, N., and Kitagawa, H. (2011) Chondroitin 4-*O*-sulfotransferase-1 regulates the chain length of chondroitin sulfate in co-operation with chondroitin *N*-acetylgalactosaminyltransferase-2. *Biochem. J.* **434,** 321–331
24. Izumikawa, T., Koike, T., and Kitagawa, H. (2012) Chondroitin 4-*O*-sulfotransferase-2 regulates the number of chondroitin sulfate chains initiated by chondroitin *N*-acetylgalactosaminyltransferase-1. *Biochem. J.* **441,** 697–705
25. Sakaguchi, H., Watanabe, M., Ueoka, C., Sugiyama, E., Taketomi, T., Yamada, S., and Sugahara, K. (2001) Isolation of reducing oligosaccharide chains from the chondroitin/dermatan sulfate-protein linkage region and preparation of analytical probes by fluorescent labeling with 2-aminobenzamide. *J. Biochem.* **129**, 107–118
26. Kitagawa, H., Tanaka, Y., Tsuchida, K., Goto, F., Ogawa, T., Lidholt, K., Lindahl, U., and Sugahara, K. (1995) *N*-Acetylgalactosamine (GalNAc) transfer to the common carbohydrate-protein linkage region of sulfated glycosaminoglycans. Identification of UDP-GalNAc:chondro-oligosaccharide α-*N*-acetylgalactosaminyltransferase in fetal bovine serum. *J. Biol. Chem.* **270,** 22190 –22195
27. Kitagawa, H., Tone, Y., Tamura, J., Neumann, K. W., Ogawa, T., Oka, S., Kawasaki, T., and Sugahara, K. (1998) Molecular cloning and expression of glucuronyltransferase I involved in the biosynthesis of the glycosaminoglycan-protein linkage region of proteoglycans. *J. Biol. Chem.* **273,** 6615– 6618
28. Ishikawa, H. O., Xu, A., Ogura, E., Manning, G., and Irvine, K. D. (2012) The Raine syndrome protein FAM20C is a Golgi kinase that phosphorylates bio-mineralization proteins. *PLoS One* **7,** e42988
29. Pedersen, L. C., Tsuchida, K., Kitagawa, H., Sugahara, K., Darden, T. A., and Negishi, M. (2000) Heparan/chondroitin sulfate biosynthesis. Structure and mechanism of human glucuronyltransferase I. *J. Biol. Chem.* **275,** 34580 –34585
30. Pedersen, L. C., Darden, T. A., and Negishi, M. (2002) Crystal structure of β1,3-glucuronyltransferase I in complex with active donor substrate UDP-GlcUA. *J. Biol. Chem.* **277,** 21869 –21873
31. McCormick, C., Duncan, G., Goutsos, K. T., and Tufaro, F. (2000) The putative tumor suppressors EXT1 and EXT2 form a stable complex that accumulates in the Golgi apparatus and catalyze the synthesis of heparan sulfate. *Proc. Natl. Acad. Sci. U.S.A.* **97,** 668 – 673
32. Venkatesan, N., Barré, L., Benani, A., Netter, P., Magdalou, J., Fournel-Gigleux, S., and Ouzzine, M. (2004) Stimulation of proteoglycan synthesis by glucuronosyltransferase-I gene delivery: a strategy to promote cartilage repair. *Proc. Natl. Acad. Sci. U.S.A.* **101,** 18087–18092
33. Nadanaka, S., Kagiyama, S., and Kitagawa, H. (2013) Roles of EXTL2, a member of the EXT family of tumour suppressors, in liver injury and regeneration processes. *Biochem. J.* **454,** 133–145
34. Purnomo, E., Emoto, N., Nugrahaningsih, D. A., Nakayama, K., Yagi, K., Heiden, S., Nadanaka, S., Kitagawa, H., and Hirata, K. (2013) Glycosaminoglycan overproduction in the aorta increases aortic calcification in murine chronic kidney disease. *J. Am. Heart Assoc.* **2,** e000405
35. Nadanaka, S., and Kitagawa, H. (2008) Heparan sulphate biosynthesis and disease. *J. Biochem.* **144,** 7–14